2006

# Aberration-free negative-refractive-index lens

Jiajun Chen
*University of New Orleans*

Cosmin Radu
*University of New Orleans*

Ashok Puri
*University of New Orleans*



## Recommended Citation

Appl. Phys. Lett. 86, 071119 (2006)

# Aberration-free negative-refractive-index lens

Jiajun Chen,[a)] Cosmin Radu,[a)] and Ashok Puri[b)]
*Department of Physics, University of New Orleans, New Orleans, Louisiana 70148*

(Received 10 August 2005; accepted 15 January 2006; published online 16 February 2006)

The aberrations of a spherical lens composed of left-handed materials are studied in this letter. Five Seidel aberrations (spherical, coma, astigmatism, field curvature, and distortion) as a function of the refractive index $n$ and shape factor $q$ of the lens are considered. Our numerical calculations show that the negative refractive index gives much larger windows of small values of aberrations than the positive index, which will significantly enhance the flexibility for the design of an optical lens. Two possible regions with optimized aberrations are proposed: $n=-1$, $q=-2.2$ and $n=-0.81$ and $q=0.83$. © *2006 American Institute of Physics*. [DOI: 10.1063/1.2174087]

Materials with simultaneously negative dielectric permittivity and magnetic permeability are called left-handed materials (LHM), in which the phase velocity of the light wave propagating is pointed in the opposite direction of the energy flow, namely, the Poynting vector is antiparallel to the wave vector. Thus, these materials possess a negative refractive index (NRI). The possibility of the existence of such materials was first point out by Veselago.[1] The successful fabrication of LHM by using photonic crystals or composite metamaterials has triggered intensive investigation on designing microwave and optical elements.[2–9] These engineered composites enable a refractive index less than one and even somewhat close to zero. Most of the engineered composites are for the microwave frequencies. In recent publications,[8,9] researchers show that nanofabricated materials can provide negative refractive index for visible frequencies. The simulation results also show that the refractive index can be $-1$ for porous alumina with infiltrated silver.[9] In comparison to traditional lenses, it is much easier to construct a nonspherical surface by using photonic crystals or composite materials. Among all these optical elements, the perfect lens,[2,10,11] actually a flat lens with a refractive index equal to $-1$, has been studied intensively due to its exceptional focusing ability by which a resolution exceeding diffraction limit is possible. However, it can operate only when the source is close to the lens. But for the practical applications, such as telescopes and microwave communications, focusing distant radiation is needed. In order to focus a farfield radiation, the NRI lens with a concave surface is generally used. Because the asymmetry of the refractive index with respect to the positive and negative value of $n$, the NRI lenses have very different focusing properties from the positive one. Schurig *et al.* recently investigated the five Seidel aberrations of the NRI lens.[12] They noted that the elimination of more aberrations is possible by using NRI lenses. They set the value of $q$ to eliminate one of the five aberrations first, and evaluated the remaining aberrations as a function of the index of refraction. This strategy does not balance all the aberrations. In order to minimize all the aberrations simultaneously, in this paper we use a numerical method to screen all the possible values of the shape factor $q$ and the refractive index $n$. We present contour maps of various aberrations as a function of $q$ and $n$ and obtain values that optimize lens aberrations.

Gaussian optics is generally used for the paraxial rays from a spherical lens. However, the paraxial approximation, $\sin\theta\approx\theta$, is unsatisfactory if the rays from the periphery of a lens are considered. In order to obtain an accurate approximation, the third order of the approximation is considered, $\sin\theta\approx\theta-\theta/3!$. Figure 1 shows a basic configuration used for the aberration calculation. As the radius of the spherical surface approach to infinite $n_1$ is a vacuum and $n_2=-1$, a lens with perfect focusing ability is constructed. A real perfect lens has two flat surfaces, thus the thickness of the lens restricts the focus distance.[10] A flat slab lens with NRI other than $-1$ will possess spherical aberrations. By calculating the conjugate points for a single refracting interface, in which the third-order expression

$$\frac{n_1}{s_0}+\frac{n_2}{s_i}=\frac{n_2-n_1}{R}+h^2\left[\frac{n_1}{2s_0}\left(\frac{1}{s_0}+\frac{1}{R}\right)^2+\frac{n_2}{2s_i}\left(\frac{1}{R}-\frac{1}{s_i}\right)^2\right] \tag{1}$$

was used, a deviation proportional to $h^2$ is measured from the first-order theory,[13] where $s_o$ and $s_i$ are the source position and the image position, respectively. The relation between the spherical aberrations and the refractive index is shown in Fig. 2, in which the object distance $s_o$ is assumed to be 1 and the maximum distance above the axis, $h$, is 0.1, 0.4, and 0.8, respectively. The spherical aberration is observed when the refractive index deviates from $-1$. It is important to note that the spherical aberration maintains a value of 1 when the refractive index is in the range of values near 0. This is because total reflection occurs for a large value of $h$ due to the

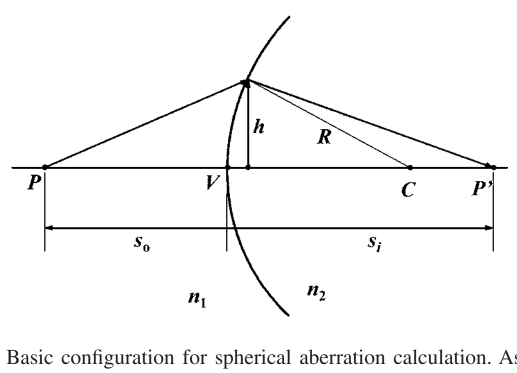


FIG. 1. Basic configuration for spherical aberration calculation. As the diameter of the spherical surface approaches infinity, $n_1=1$ and $n_2=-1$, a "perfect lens" is constructed.

[a)]Also at: Advanced Materials Research Institute, University of New Orleans, New Orleans, Louisiana 70148

[b)]Author to whom correspondence should be addressed; electronic mail: apuri@uno.edu

 

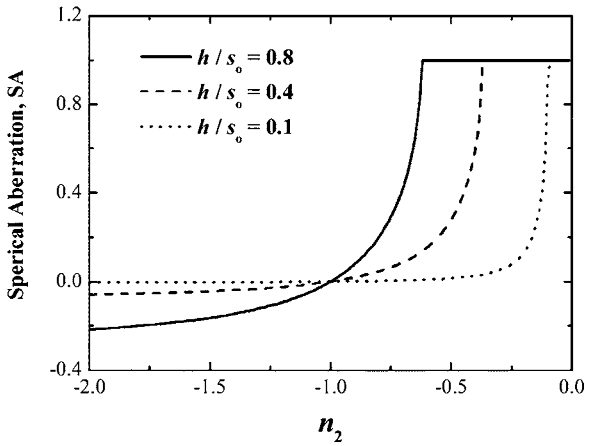


FIG. 2. The spherical aberration as a function of refractive index $n$. The object distance $s_o$ is assumed to be 1 and the maximum distance above the axis, $h$, is 0.8.

strong refraction effect for small values of $n_2$, which prevents the ray with large $h$ to transmit the interface.

As the third-order term is included, several aberrations arise for the monochromatic optics. The monochromatic imaging quality of a lens can be characterized by the five aberrations: spherical, coma, astigmatism, field curvature, and distortion, which are known as five Seidel aberrations. These corrections to the simple Gaussian optical formulas are calculated from a third-order expansion of the deviation of a wave front from spherical. Normally, a spherical wave front converges to an ideal point focus in ray optics. For an object point on the optical axis, the deviation from ideal spherical case is proportional to $h^4$,[13]

$$\text{Aberration}(Q) = -\frac{h^4}{8}\left[\frac{n_1}{s_0}\left(\frac{1}{s_0}+\frac{1}{R}\right)^2 + \frac{n_2}{s_i}\left(\frac{1}{s_i}-\frac{1}{R}\right)^2\right]. \tag{2}$$

The construction used for an off-axis object point is shown in Fig. 3.[14] $P$ is the source point and $P'$ is the image point. A general case of $Q$ is considered in this calculation, in which $Q$ is not collinear with the point $B$. The aberration of $PQP'$ should be equal to the optical path difference between the ray paths $PQP'$ and $POP'$, and it can be calculated by subtracting the two optical path differences:

$$(PQP' - PBP')_{\text{optical}} = c(BQ)^4 = c(\rho')^4,$$

and

$$(POP' - PBP')_{\text{optical}} = c(BO)^4 = c(b)^4,$$

where $c$ is proportional constant and $\rho'$ and $b$ are given in Fig. 3(b). Therefore,

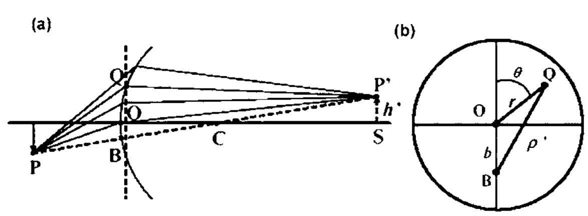


FIG. 3. Configuration for the five Seidel aberrations calculation. (a) Light trace diagram. (b) End-on view of the imaging situation along the axis. $P$ and $P'$ are the object and image position, respectively. $r$ is the aperture stop coordinate vector and $h'$ is the image plane coordinate vector.

$$\text{Aberration}(Q) = c\rho'^4 - cb^4. \tag{3}$$

By using the trigonometric relationship (cosine law), $\rho'^2 = r^2 + b^2 + 2rb\cos\theta$ and the proportionality between $b$ and $h'$, $b = kh'$ ($k$ is a constant), the Seidel aberration equation is written as

$$\begin{aligned}\text{Aberration}(Q) = {} & C_{040}r^4 + C_{131}rh'\cos\theta \\ & + C_{222}r^2h'^2\cos^2\theta + C_{220}r^2b^2 \\ & + C_{311}rh'^3\cos\theta.\end{aligned} \tag{4}$$

The coefficients quantify the nonideal focusing properties of an optical element for a given object and image position. These coefficients are the five Seidel aberrations: spherical, coma, astigmatism, field curvature, and distortion. They can be written by the refractive index ($n$), the position factor ($p$), the shape factor ($q$), and the focal length ($f'$), the definitions of which were given by Mahajan.[15] For most applications in reality, such as telescopes and microwave communications, we would like to focus the radiation from the object at infinite position. In this case, $p=-1$ and $f'=1$, and the five coefficients are the function of refractive index $n$ and the shape factor $q$:

$$C_{040} = -\frac{n^3 + (n-1)^2(3n+2) - 4(n+1)(n-1)q + (n+2)q^2}{32n(n-1)^2}, \tag{5a}$$

$$C_{131} = \frac{(2n+1)(n-1) - (n+1)q}{4n(n-1)}, \tag{5b}$$

$$C_{222} = -\frac{1}{2}, \tag{5c}$$

$$C_{220} = -\frac{(n+1)}{4n}, \tag{5d}$$

$$C_{311} = 0. \tag{5e}$$

The astigmatism and distortion are independent of the refractive index and the shape factor and maintain values of $-0.5$ and 0, respectively. Field curvature $C_{220}$ is independent of the shape factor of the lens, and only when $n=-1$, the field curvature is zero. It is impossible to eliminate field curvature when $n$ is positive. Furthermore, the field curvature goes to infinity when $n=0$. Schurig *et al.*[12] bent the lens (change shape factor) to eliminate one aberration and evaluate the others. If coma $C_{131}$ is zero, the shape factor is given by $q=(2n+1)(n-1)/(n+1)$. And this will cause the spherical aberration goes to infinity for $n=-1$. For a lens with zero spherical aberration, the shape factor can be written by

$$q = \frac{4n^2 - 4 \pm 2\sqrt{n^2 - 4n^3}}{2(n+2)}, \tag{6}$$

which requires $n \leqslant 1/4$. This means it is impossible to eliminate spherical aberration when $n > 1/4$. Thus, the spherical aberration and curvature can be eliminated simultaneously with a relatively small coma ($C_{131}=0.25$) when $n=-1$, and $q=\pm\sqrt{5}$. However, these analyses do not examine all the situations with respect to different shape factors $q$ and refractive indexes $n$, respectively. In order to evaluate all the possible situations and balance these aberrations, we numeri-

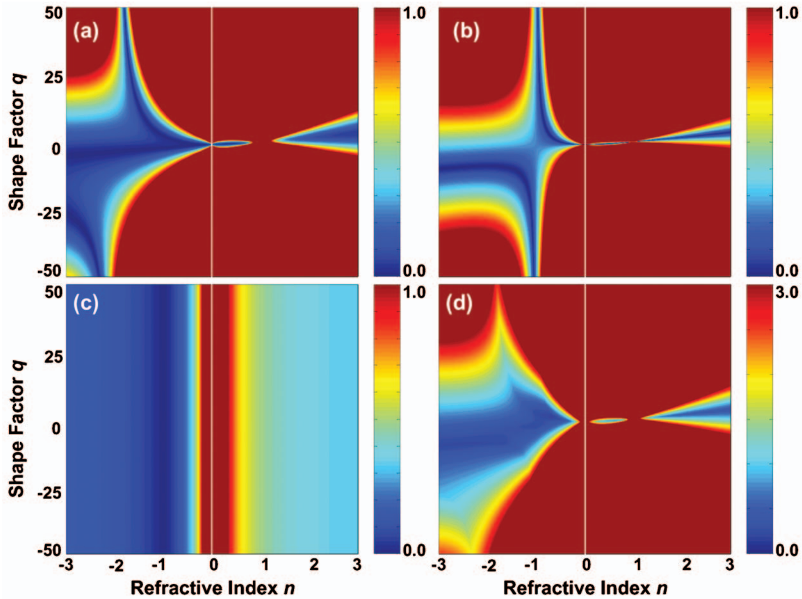


FIG. 4. (Color) Numerical calculated coefficients of the spherical aberration $C_{040}$ (a), coma $C_{131}$ (b), curvature $C_{220}$ (c), and the sum of the three aberrations $|C_{040}|+|C_{131}|+|C_{220}|$ (d) as a function of the shape factor $q$ and refractive index $n$. The values of the color bars for the spherical aberration, coma, and field curvature range from 0 (navy blue) to 1 (garnet), and the value for the sum spans from 0 to 3.

cally calculate the dependence of the aberration coefficients on the shape factor and the refractive index, namely, we expand our evaluation of aberrations to the $n-q$ plane. The results for the spherical aberration, coma, and curvature are shown in Figs. 4(a)–4(c) in a color-coded scheme. For all of these aberrations, the negative index gives much larger windows of small aberrations (navy blue areas) than those given by the positive refractive index. A better method to minimize the aberrations simultaneously is to evaluate the dependence of the sum of the absolute values of aberrations, $C_{\text{total}}=|C_{040}|+|C_{131}|+|C_{220}|$, on the parameters ($q$ and $n$). The values of $C_{\text{total}}$ with respect to $q$ and $n$ are plotted in Fig. 4(d). Not surprisingly, the negative refractive index has a much larger window of small aberrations. This asymmetry implies much more flexibility of the lens design by using the negative refractive index. The detailed contour map of the areas with small aberrations is also plotted in Fig. 5. We should concentrate on small absolute values of index, because a large index will yield strong reflection due to the impedance mismatch. The numerical results show that there are two minimum values of $C_{\text{total}}$ with a small absolute index: $C_{\text{total}}=0.25$ ($n=-1$, $q=-2.2$) and $C_{\text{total}}=0.22$ ($n=-0.81$, $q=0.83$). As $q=-2.2$ and $n=-1$, the three aberrations are optimized: $C_{040}=-0.0001$, $C_{131}=0.25$, $C_{220}=0$, which is corresponding to the analytical result shown before. The situation that $n=-0.81$, $q=0.83$ is another possible selection for optimizing $C_{\text{total}}$, for which $C_{040}=0.0004$, $C_{131}=0.1644$, and $C_{220}=0.0586$. Thus, $q=-2.2$ implies curvature ratio $R_1/R_2=(q-1)/(q+1)\approx 2.7$ (concavo-convex), and $q=0.83$ gives $R_1/R_2\approx -0.093$ (a biconcave or biconvex lens).

In summary, the Seidel aberrations, including spherical, coma, astigmatism, field curvature, and distortion, are investigated for the lens with a negative refractive index. The numerical calculation results show that the negative refractive index gives much larger windows of small values of aberrations, which will significantly enhance the design flexibility of an optical lens. Two possible areas with minimized aberrations are proposed: $n=-1$, $q=-2.2$ and $n=-0.81$ and $q=0.83$.

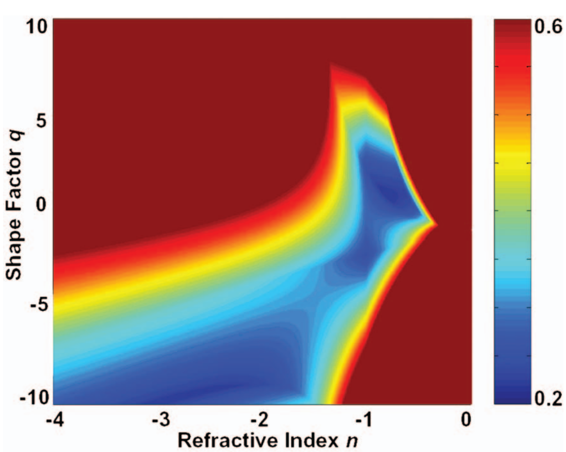


FIG. 5. (Color) Detailed contour map of the area with small values of the sum of the three aberrations $C_{\text{total}}=|C_{040}|+|C_{131}|+|C_{220}|$. There are two minimums near the small refractive index area ($|n|<2$): $C_{\text{total}}=0.22$ for $n=-0.81$ and $q=0.83$; $C_{\text{total}}=0.25$ for $n=-1$ and $q=-2.2$. In order to give the details, the range of the color bar is shrunk to the values from 0.2 to 0.6.


[1]V. G. Veselago, Sov. Phys. Usp. **10**, 509 (1968).
[2]P. V. Parimi, W. T. Lu, P. Vodo, and S. Sridhar, Nature (London) **426**, 404 (2003).
[3]E. Cubukcu, K. Aydin, E. Ozbay, S. Foteinopoulou, and C. M. Soukoulis, Nature (London) **423**, 604 (2003).
[4]P. Vodo, P. V. Parimi, W. T. Lu, and S. Sridhar, Appl. Phys. Lett. **86**, 201108 (2005).
[5]R. A. Shelby, D. R. Smith, and S. Schultz, Science **292**, 77 (2001).
[6]S. Zhang, W. Fan, N. C. Panoiu, K. J. Malloy, R. M. Osgood, and S. R. J. Brueck, Phys. Rev. Lett. **95**, 137404 (2005).
[7]P. V. Parimi, W. T. Lu, P. Vodo, J. B. Sokoloff, and S. Sridhar, Phys. Rev. Lett. **92**, 127401 (2004).
[8]X. Ao and S. He, Appl. Phys. Lett. **87**, 101112 (2005).
[9]A. N. Grigorenko, A. K. Geim, H. F. Gleeson, Y. Zhang, A. A. Firsov, I. Y. Khrushchev, and J. Petrovic, Nature (London) **438**, 335 (2005).
[10]J. B. Pendry, Phys. Rev. Lett. **85**, 3966 (2000).
[11]C. Luo, S. Johnson, J. Joannopoulos, and J. Pendry, Phys. Rev. B **65**, 201104 (2002).
[12]D. Schurig and D. R. Smith, Phys. Rev. E **70**, 065601 (2004).
[13]E. Hecht, *Optics*, 3rd ed. (Addison-Wesley, Reading, MA, 1998).
[14]F. L. Pedrotti and L. S. Pedrotti, *Introduction to Optics*, 2nd ed. (Prentice–Hall, Englewood Cliffs, NJ, 1992).
[15]V. N. Mahajan, *Optical Imaging and Aberrations*, 1st ed. (SPIE, Bellingham, WA, 1998), Vol. I.